

1 **The *sek-1* p38 MAP kinase pathway regulates Gq signaling in *C. elegans***

2

3

4 Jill M. Hoyt, Samuel K. Wilson, Madhuri Kasa, Jeremy S. Rise,

5 Irimi Topalidou, Michael Ailion

6

7 Department of Biochemistry, University of Washington, Seattle, WA, 98195

8

9 Running Title: *sek-1* regulates Gq signaling

10

11

12 key words: p38 MAPK pathway, Gq signaling, animal behavior, *C. elegans*

13

14 Corresponding author:

15 Michael Ailion

16 Department of Biochemistry

17 University of Washington

18 Box 357350

19 1705 NE Pacific St

20 Seattle, WA 98195

21 Phone: 206-685-0111

22 email: mailion@uw.edu

23

24 **Abstract**

25 Gq is a heterotrimeric G protein that is widely expressed in neurons and
26 regulates neuronal activity. To identify pathways regulating neuronal Gq signaling we
27 performed a forward genetic screen in *Caenorhabditis elegans* for suppressors of
28 activated Gq. One of the suppressors is an allele of *sek-1*, which encodes a mitogen-
29 activated protein kinase kinase (MAPKK) in the p38 MAPK pathway. Here we show that
30 *sek-1* mutants have a slow locomotion rate and that *sek-1* acts in acetylcholine neurons
31 to regulate both locomotion and Gq signaling. Furthermore, we find that *sek-1* acts in
32 mature neurons to regulate locomotion. Using genetic and behavioral approaches we
33 demonstrate that other components of the p38 MAPK pathway also play a positive role
34 in regulating locomotion and Gq signaling. Finally, we find that mutants in the *sek-1* p38
35 MAPK pathway partially suppress an activated mutant of the sodium leak channel NCA-
36 1/NALCN, a downstream target of Gq signaling. Our results suggest that the *sek-1* p38
37 pathway may modulate the output of Gq signaling through NCA-1.

38

39 Introduction

40 Gq is a widely expressed heterotrimeric G protein that regulates a variety of
41 biological processes ranging from neurotransmission to cardiovascular pathophysiology
42 (Sánchez-Fernández et al., 2014). In the canonical Gq pathway, Gq activates
43 phospholipase C β (PLC β), which cleaves phosphatidylinositol 4,5-bisphosphate (PIP₂)
44 into the second messengers diacylglycerol (DAG) and inositol trisphosphate (IP₃)
45 (Rhee, 2001). In addition to PLC β , other Gq effectors have been identified including
46 kinases, such as protein kinase C ζ (PKC ζ) and Bruton's tyrosine kinase (Btk) (Bence et
47 al., 1997; García-Hoz et al., 2010), and guanine nucleotide exchange factors (GEFs) for
48 the small GTPase Rho, such as Trio (Williams et al., 2007; Vaqué et al., 2013). These
49 noncanonical effectors bridge the activation of Gq to other cellular signaling cascades.

50 In order to study noncanonical pathways downstream of Gq, we used the nematode
51 *C. elegans* which has a single G α q homolog (EGL-30) and conservation of the other
52 components of the Gq signaling pathway (Koelle, 2016). In neurons, EGL-30 signals
53 through EGL-8 (PLC β) (Lackner et al., 1999) and UNC-73 (ortholog of Trio RhoGEF)
54 (Williams et al., 2007). UNC-73 activates RHO-1 (ortholog of RhoA), which has been
55 shown to enhance neurotransmitter release through both diacylglycerol kinase (DGK-1)-
56 dependent and DGK-1-independent pathways (McMullan et al., 2006).

57 To identify additional signaling pathways that modulate Gq signaling, we screened
58 for suppressors of the activated Gq mutant *egl-30(tg26)* (Doi and Iwasaki, 2002),
59 hereafter referred to as *egl-30(gf)*. *egl-30(gf)* mutant animals exhibit hyperactive
60 locomotion and a “loopy” posture in which worms have exaggerated, deep body bends
61 and loop onto themselves (Bastiani et al., 2003). Here we identify one of the

62 suppressors as a deletion allele in the gene *sek-1*. SEK-1 is a mitogen-activated protein
63 kinase kinase (MAPKK), the *C. elegans* ortholog of mammalian MKK3/6 in the p38
64 MAPK pathway (Tanaka-Hino et al., 2002). The p38 MAPK pathway has been best
65 characterized as a pathway activated by a variety of cellular stresses and inflammatory
66 cytokines (Kyriakis and Avruch, 2012). However, the p38 MAPK pathway has also been
67 shown to be activated downstream of a G protein-coupled receptor in rat neurons
68 (Huang et al., 2004). Btk, a member of the Tec family of tyrosine kinases, has been
69 shown to act downstream of Gq to activate the p38 MAPK pathway (Bence et al., 1997),
70 but *C. elegans* lacks Btk and other Tec family members (Plowman et al., 1999).

71 SEK-1 is activated by the MAPKKK NSY-1 (ortholog of ASK1) and activates the p38
72 MAPKs PMK-1 and PMK-2 (Andrusiak and Jin, 2016). The p38 MAPK pathway
73 consisting of NSY-1/SEK-1/PMK-1 is required for innate immunity in *C. elegans* (Kim et
74 al., 2002). NSY-1 and SEK-1 are also required for the specification of the asymmetric
75 AWC olfactory neurons (Sagasti et al., 2001; Tanaka-Hino et al., 2002); the p38
76 orthologs PMK-1 and PMK-2 function redundantly in AWC specification (Pagano et al.,
77 2015). For both innate immunity and AWC specification, the p38 MAPK pathway acts
78 downstream of the adaptor protein TIR-1 (an ortholog of SARM) (Couillault et al., 2004;
79 Chuang and Bargmann, 2005). Here we show that the TIR-1/NSY-1/SEK-1/PMK-1
80 PMK-2 signaling module also acts to regulate locomotion downstream of Gq signaling.

81

82 **Materials and Methods**

83 ***C. elegans* strains and maintenance**

84 All strains were cultured using standard methods and maintained at 20°C
85 (Brenner, 1974). The *sek-1(yak42)* mutant was isolated from an ENU mutagenesis
86 suppressor screen of the activated Gq mutant *egl-30(tg26)* (“*egl-30(gf)*”) (Ailion et al.,
87 2014). *sek-1(yak42)* was outcrossed away from *egl-30(gf)* before further analysis.
88 Double mutant strains were constructed using standard methods (Fay, 2006) often with
89 linked fluorescent markers (Frokjaer-Jensen et al., 2014) to balance mutations with
90 subtle visible phenotypes. Table S1 contains all the strains used in this study.

91

92 **Mapping**

93 *yak42* was mapped using the slow locomotion phenotype and its *egl-30(gf)*
94 suppression phenotype. *yak42* was initially mapped to Chromosome X using strains
95 EG1000 and EG1020, which carry visible marker mutations. These experiments
96 showed that *yak42* was linked to *lon-2*, but at least several map units away. *yak42* was
97 further mapped to about one map unit (m.u.) away from the red fluorescent insertion
98 marker *oxTi668* which is located at +0.19 m.u. on Chromosome X.

99

100 **Whole-genome sequencing**

101 Strain XZ1233 *egl-30(tg26); yak42* was used for whole-genome sequencing to
102 identify candidate *yak42* mutations. XZ1233 was constructed by crossing a 2X
103 outcrossed *yak42* strain back to *egl-30(tg26)*. Thus, in XZ1233, *yak42* has been
104 outcrossed 3X from its original isolate. DNA was isolated from XZ1233 and purified
105 according to the Hobert Lab protocol (<http://hobertlab.org/whole-genome-sequencing/>).
106 Ion Torrent sequencing was performed at the University of Utah DNA Sequencing Core

107 Facility. The resulting data contained 10,063,209 reads of a mean read length of 144
108 bases, resulting in about 14X average coverage of the *C. elegans* genome. The
109 sequencing data were uploaded to the CloudMap pipeline on the Galaxy platform
110 (Minevich et al., 2012) and SNPs and indels were identified. We filtered out
111 polymorphisms found in other strains we sequenced, leaving us with 605 homozygous
112 mutations. Chromosome X contained 94 mutations: 55 SNPs and 39 indels. Of these,
113 four SNPs were non-synonymous mutations in protein-coding genes, but only 2 were
114 within 5 m.u. of *oxTi668*. However, we were unable to identify *yak42* from the candidate
115 polymorphisms located near *oxTi668*. Transgenic expression of the most promising
116 candidate *pcyt-1* (located at -1.49 m.u.) did not rescue *yak42*. Instead, to identify
117 possible deletions, we scrolled through 2 MB of aligned reads on the UCSC Genome
118 Browser starting at -4.38 m.u. and working towards the middle of the chromosome (0
119 m.u.), looking for regions that lacked sequence coverage. We found a 3713 bp deletion
120 that was subsequently confirmed to be the *yak42* causal mutation, affecting the gene
121 *sek-1* located at -1.14 m.u.

122

123 ***Locomotion assays***

124 Locomotion assay plates were made by seeding 10 cm nematode growth
125 medium plates with 150 μ l of an OP50 (a strain of *E. coli*) stock culture, spread with
126 sterile glass beads to cover the entire plate. Bacterial lawns were grown at room
127 temperature (22.5°C -24.5°C) for 24 hrs and then stored at 4°C until needed. All
128 locomotion assays were performed on first day adults. L4 stage larvae were picked the
129 day before the assay and the experimenter was blind to the genotypes of the strains

130 assayed. For experiments on strains carrying extrachromosomal arrays, the *sek-1(km4)*
131 control worms were animals that had lost the array from the same plate.

132 Body bends assays were performed as described (Miller et al., 1999). The
133 locomotion assay plate was brought to room temperature (22.5°C -24.5°C). All strains in
134 an experiment were assayed on the same assay plate. A single animal was picked onto
135 the plate, the plate lid was returned, and the animal recovered for 30 s. Body bends
136 were then counted for one minute. A body bend was counted each time the worm's tail
137 reached the minimum or maximum amplitude of the sine wave. For experiments with
138 *egl-8*, *unc-73*, and *rund-1*, worms were allowed a minimal recovery period (until the
139 worms started moving forward, 5 sec maximum) prior to counting body bends.

140 For the heat shock experiment, plates of first-day adults were parafilmmed and
141 heatshocked in a 34°C water bath for 1 hr. Plates were then un-parafilmmed and
142 incubated at 20°C for five hours before performing body bend assays.

143 Radial locomotion assays were performed by first bringing the locomotion assay
144 plates to room temperature. Animals were picked to the middle of the plate, the plate
145 taped shut, and an x was marked on the lid above where the animals were placed.
146 Assay plates were then incubated at 20°C for 20 hr and the distances of the worms from
147 the starting point were measured.

148 Quantitative analysis of the waveform of worm tracks was performed by first
149 bringing the locomotion assay plate to room temperature. One strain at a time, five
150 animals were placed on the plate and allowed to roam for 2-5 min. We then took five
151 pictures of each animal's tracks following forward locomotion. Track pictures were taken
152 at 40X on a Nikon SMZ18 microscope with the DS-L3 camera control system. This

153 process was repeated for all strains per experiment set. Worm track pictures were
154 processed using ImageJ. Tracks were straightened with the segmented line tool and
155 pictures converted to grayscale. Period and 2X amplitude were measured freehand
156 using the line tool. For each worm, five period/amplitude ratios were calculated from
157 each of the five straightened tracks. The ratios were averaged for each worm and these
158 averages were averaged for each strain.

159

160 ***C. elegans* pictures**

161 Pictures of worms were taken at 60X on a Nikon SMZ18 microscope with the DS-
162 L3 camera control system. The worms were age-matched as first day adults and each
163 experiment set was photographed on the same locomotion assay plate (assay plate
164 preparation described above). The images were processed using ImageJ and were
165 rotated, cropped, and converted to grayscale.

166

167 ***Molecular biology***

168 Plasmids were constructed using the Gateway cloning system (Invitrogen).
169 Plasmids and primers used are found in Table S2. The *sek-1* cDNA was amplified by
170 RT-PCR from worm RNA and cloned into a Gateway entry vector. To check for proper
171 expression of *sek-1*, an operon GFP was included in expression constructs with the
172 following template: (promoter)p::*sek-1*(cDNA)::*tbb-2utr*::*gpd-2 operon*::*GFP*::*H2B*::*cye-*
173 *1utr* (Frøkjær-Jensen et al., 2012). This resulted in untagged SEK-1, but expression
174 could be monitored by GFP expression.

175

176 ***Injections***

177 *C. elegans* strains with extrachromosomal arrays were generated by standard
178 methods (Mello et al., 1991). Injection mixes were made with a final total concentration
179 of 100 ng/ μ L DNA. Constructs were injected at 5 ng/ μ L, injection markers at 5 ng/ μ L,
180 and the carrier DNA Litmus 38i at 90 ng/ μ L. Multiple lines of animals carrying
181 extrachromosomal arrays were isolated and had similar behaviors as observed by eye.
182 The line with the highest transmittance of the array was assayed.

183

184 ***Statistical analysis***

185 At the beginning of the project, a power study was conducted on pilot body bend
186 assays using wild type and *sek-1(yak42)* worms. To achieve a power of 0.95, it was
187 calculated that 17 animals should be assayed per experiment. Data were analyzed to
188 check if normally distributed (using the D'Agostino-Pearson and Shapiro-Wilk normality
189 tests) and then subjected to the appropriate analysis using GraphPad Prism 5. For data
190 sets with three or more groups, if the data were normal they were analyzed with a one-
191 way ANOVA; if not, with a Kruskal-Wallis test. Post-hoc tests were used to compare
192 appropriate data sets within an experiment. Reported p-values are corrected. Table S3
193 contains the statistical tests for each experiment. $p < 0.05 = *$; $p < 0.01 = **$; $p < 0.001 = ***$.

194

195 ***Reagent and Data Availability***

196 Strains and plasmids are shown in Table S1 and Table S2 and are available from
197 the *Caenorhabditis* Genetics Center (CGC) or upon request. The authors state that all

198 data necessary for confirming the conclusions presented in the article are represented
199 fully within the article and Supplemental Material.

200

201 **Results**

202 ***sek-1* suppresses activated Gq**

203 To identify downstream effectors of Gq, we performed a forward genetic screen
204 for suppressors of the activated Gq mutant, *egl-30(tg26)* (Doi and Iwasaki, 2002),
205 referred to here as *egl-30(gf)*. *egl-30(gf)* worms are small, hyperactive, and have a
206 “loopy” posture characterized by a high-amplitude waveform (Figure 1B). Thus, we
207 screened for worms that are larger, less hyperactive, and less loopy. We isolated a
208 recessive suppressor, *yak42*, and mapped it to the middle of Chromosome X (see
209 Materials and Methods). Whole-genome sequencing revealed that *yak42* carries a large
210 deletion of the *sek-1* gene from upstream of the start codon to exon 4 (Figure 1A).
211 *yak42* also failed to complement *sek-1(km4)*, a previously published *sek-1* deletion
212 allele (Figure 1A) (Tanaka-Hino et al., 2002).

213 *egl-30(gf)* double mutants with either *sek-1(yak42)* or *sek-1(km4)* are bigger than
214 *egl-30(gf)* worms (Figure 1B), not hyperactive (Figure 1C). and have a tendency to kink
215 when moving backward. Additionally, both *sek-1* mutations suppress the loopy
216 waveform phenotype (Figure S1A, B).

217 *sek-1(yak42)* was outcrossed from *egl-30(gf)* and assayed for locomotion
218 defects. Both the *sek-1(yak42)* and *sek-1(km4)* mutants are coordinated but move more
219 slowly than wild-type (Figure 1D). *sek-1(ag1)*, a point mutation in exon 5 (Kim et al.,
220 2002), also causes a similar slow locomotion phenotype (Figure S1C). To test whether

221 the *egl-30(gf)* suppression phenotype might be an indirect effect of the slow locomotion
222 of a *sek-1* mutant, we built an *egl-30(gf)* double mutant with a mutation in *unc-82*, a
223 gene required for normal muscle structure. *unc-82* mutants are coordinated but move
224 slowly, similar to a *sek-1* mutant (Hoppe et al., 2010). However, although an *egl-30(gf)*
225 *unc-82(e1220)* double mutant moves more slowly than *egl-30(gf)*, it is still small and
226 loopy (Figure 1B). Thus, *sek-1* appears to be a specific suppressor of multiple
227 phenotypes of the *egl-30(gf)* mutant, suggesting that *sek-1* regulates locomotion and
228 acts downstream of Gq.

229 EGL-30/Gαq is negatively regulated by GOA-1, the worm Gao/i ortholog (Hajdu-
230 Cronin et al., 1999). We tested whether *sek-1* also suppresses a *goa-1* loss-of-function
231 mutant that causes a hyperactive phenotype similar to *egl-30(gf)*. Indeed, *sek-1(km4)*
232 suppresses *goa-1(sa734)* (Figure S1D). One downstream effector of GOA-1 is the DAG
233 kinase DGK-1 (DGKΘ ortholog) that inhibits DAG-dependent functions such as synaptic
234 vesicle release (Nurrish et al. 1999; Miller et al. 1999). *dgk-1(sy428)* animals are
235 hyperactive, but *sek-1(km4)* does not suppress *dgk-1*. Rather, the *sek-1 dgk-1* double
236 mutant is uncoordinated and looks like neither *sek-1* nor *dgk-1* mutants, confounding
237 the interpretation of how *sek-1* genetically interacts with *dgk-1*.

238

239 ***sek-1* acts in mature acetylcholine neurons**

240 *egl-30* is widely expressed and acts in neurons to regulate locomotion (Lackner
241 et al., 1999), so it is possible that *sek-1* also acts in neurons to regulate Gq signaling.
242 *sek-1* is expressed in neurons, intestine, and several other tissues (Tanaka-Hino et al.,

243 2002) and has been shown to function in GABA neurons to possibly promote GABA
244 release (Vashlishan et al., 2008).

245 To identify the cell type responsible for the *sek-1* locomotion phenotypes, we
246 expressed the wild-type *sek-1* cDNA under different cell-specific promoters and tested
247 for transgenic rescue of a *sek-1* null mutant. Expression of *sek-1* in all neurons (using
248 the *unc-119* promoter) or in acetylcholine neurons (using *unc-17p*) was sufficient to
249 rescue the *sek-1* mutant slow locomotion phenotype, but expression in GABA neurons
250 (using *unc-47p*) was not sufficient to rescue (Figure 2A, B). These results indicate that
251 *sek-1* acts in acetylcholine neurons to regulate locomotion.

252 We next tested whether *sek-1* also acts in neurons to suppress *egl-30(gf)*.
253 Expression of *sek-1* under pan-neuronal and acetylcholine neuron promoters rescued
254 the *sek-1* suppression of *egl-30(gf)*. Specifically, *egl-30(gf) sek-1* double mutants
255 expressing wild-type *sek-1* in all neurons or acetylcholine neurons had a hyperactive,
256 loopy, small phenotype that resembled the *egl-30(gf)* single mutant (Figure 2C, D).
257 However, expression of *sek-1* in GABA neurons did not rescue the suppression
258 phenotype (Figure 2C, D). Together, these data show that *sek-1* acts in acetylcholine
259 and not GABA neurons to regulate both wild-type locomotion and to modulate Gq
260 signaling.

261 Because *sek-1* acts in the development of the AWC asymmetric neurons, we
262 asked whether *sek-1* also has a developmental role in regulating locomotion by testing
263 whether adult-specific *sek-1* expression (driven by a heat-shock promoter) is sufficient
264 to rescue the *sek-1* mutant. We found that *sek-1* expression in adults rescues the *sek-1*
265 slow locomotion phenotype (Figure 2E). This result indicates that *sek-1* is not required

266 for development of the locomotion circuit and instead acts in mature neurons to regulate
267 locomotion.

268

269 **The p38 MAPK pathway is a positive regulator of Gq signaling**

270 SEK-1 is the MAPKK in a p38 MAPK pathway (Tanaka-Hino et al., 2002). This
271 pathway consists of NSY-1 (MAPKKK), SEK-1 (MAPKK), and PMK-1 or PMK-2
272 (MAPKs)(Andrusiak and Jin, 2016). TIR-1 acts upstream of NSY-1. This p38 MAPK
273 signaling module has been shown to function in innate immunity and the development
274 of the AWC olfactory neurons (Chuang and Bargmann, 2005).

275 We tested whether the entire p38 MAPK and TIR-1 signaling module also
276 regulates locomotion and suppression of activated Gq. Both *tir-1(tm3036)* and *nsy-*
277 *1(ok593)* mutant animals have slow locomotion on their own and also suppress the
278 hyperactivity, deep body bends and small size of *egl-30(gf)* (Figure 3A-D; Figure S2A,
279 B). We also tested single mutants in each of the three worm p38 MAPK genes (*pmk-1*,
280 *pmk-2* and *pmk-3*) and a *pmk-2 pmk-1* double mutant. Although we found that the *pmk-*
281 *2* and *pmk-3* single mutants were slightly slow on their own, only the *pmk-2 pmk-1*
282 double mutant phenocopied *sek-1* and suppressed both the hyperactivity and deep
283 body bends of *egl-30(gf)* (Figure 3, E-G). Thus, *pmk-2* and *pmk-1* act redundantly
284 downstream of *sek-1* to suppress *egl-30(gf)*. These data suggest that the p38 MAPK
285 pathway regulates locomotion in *C. elegans* and acts genetically downstream of *egl-30*.

286 The JNK MAPK pathway, related to the p38 MAPK family, also regulates
287 locomotion in *C. elegans*. Specifically, the JNK pathway members *jkk-1* (JNK MAPKK)
288 and *jnk-1* (JNK MAPK) have been shown to act in GABA neurons to regulate

289 locomotion (Kawasaki et al., 1999). We found that the *jkk-1* and *jnk-1* single mutants
290 had slow locomotion and that the double mutants with p38 MAPK pathway members
291 exhibited an additive slow locomotion phenotype (Figure S2C). Moreover, neither *jkk-1*
292 nor *jnk-1* suppressed *egl-30(gf)* (data not shown). Thus, the JNK and p38 MAPK
293 pathways regulate locomotion independently and the JNK pathway is not involved in Gq
294 signaling.

295 We also tested the involvement of possible p38 MAPK pathway effectors. One of
296 the targets of PMK-1 is the transcription factor ATF-7 (Shivers et al., 2010). Both the *atf-*
297 *7(qd22 qd130)* loss-of-function mutant and the *atf-7(qd22)* gain-of-function mutant
298 moved slowly compared to wild-type animals (Figure S2D). However, *atf-7(qd22 qd130)*
299 did not suppress *egl-30(gf)* (data not shown), suggesting that *atf-7* is not a target of this
300 pathway or acts redundantly with other downstream p38 MAPK targets. We also tested
301 *gap-2*, the closest *C. elegans* homolog of ASK1-interacting Protein (AIP1) which
302 activates ASK1 (the ortholog of *C. elegans* NSY-1) in mammalian systems (Zhang et
303 al., 2003). A *C. elegans gap-2* mutant has no locomotion defect (Figure S2E). Finally,
304 we tested VHP-1, a phosphatase for p38 and JNK MAPKs that inhibits p38 MAPK
305 signaling (Kim et al., 2004). However, the *vhp-1(sa366)* mutant also has no locomotion
306 defect (Figure S2E).

307 *egl-30(gf)* animals are loopy and hyperactive so we tested whether increased
308 activation of the TIR-1/p38 MAPK signaling module causes similar phenotypes. The *tir-*
309 *1(ky648gf)* allele leads to a gain-of-function phenotype in the AWC neuron specification
310 (Chang et al., 2011), but does not cause a locomotion phenotype reminiscent of *egl-*
311 *30(gf)* (Figure S2F, G).

312

313 **Genetic interactions of *sek-1* with pathways acting downstream of Gq**

314 Our forward genetic screen for suppressors of *egl-30(gf)* identified mutants that
315 fall into three different categories: mutants in the canonical Gq pathway such as the
316 PLC *egl-8* (Lackner et al., 1999), mutants in the RhoGEF Trio pathway such as *unc-73*
317 (Williams et al., 2007), and mutants that affect dense-core vesicle biogenesis and
318 release (Ailion et al., 2014; Topalidou et al., 2016a).

319 To test if *sek-1* acts in these pathways we used genetic epistasis analysis. Loss-
320 of-function alleles of *egl-8(sa47)*, *unc-73(ox317)*, and *rund-1(tm3622)* have slow
321 locomotion (Figure 4A-C). Our data show that *sek-1* enhances the phenotype of *egl-8*
322 and *rund-1* single mutants, suggesting that *sek-1* does not act in the same pathway as
323 *egl-8* or *rund-1* (Figure 4A, B). By contrast, *sek-1* does not enhance the slow locomotion
324 phenotype of *unc-73* mutants (Figure 4C), suggesting that *sek-1* may act in the same
325 genetic pathway as the Trio RhoGEF *unc-73*.

326 We next tested whether *sek-1* interacts with *rho-1*, encoding the small G protein
327 activated by Trio. *rho-1* is required for viability so we could not use a loss-of-function
328 allele to test for a genetic interaction (Jantsch-Plunger et al., 2000). Instead we used an
329 integrated transgene overexpressing an activated *rho-1* mutant allele specifically in
330 acetylcholine neurons. Animals carrying this activated RHO-1 transgene, referred to
331 here as *rho-1(gf)*, have a loopy posture reminiscent of *egl-30(gf)* (McMullan et al.,
332 2006), and a decreased locomotion rate. *rho-1(gf) sek-1(km4)* double mutants had a
333 loopy body posture like *rho-1(gf)* and an even slower locomotion rate (Figure 4D, E),
334 suggesting that *sek-1* and *rho-1(gf)* mutants have additive locomotion phenotypes.

335 However, both *sek-1(km4)* and *sek-1(yak42)* suppress the slow growth rate of the *rho-*
336 *1(gf)* mutant. Because *sek-1* does not enhance *unc-73* mutants and suppresses some
337 aspects of the *rho-1(gf)* mutant, *sek-1* may modulate output of the Rho pathway, though
338 it probably is not a direct transducer of Rho signaling.

339

340 ***sek-1* and *nsy-1* partially suppress activated NCA**

341 The data above did not clarify the relationship of *sek-1* to the Rho pathway acting
342 downstream of Gq. The downstream target of this Gq-Rho pathway appears to be the
343 NCA-1 cation channel (Topalidou et al., 2016b). NCA-1 and its orthologs are sodium
344 leak channels associated with rhythmic behaviors in several organisms (Nash et al.,
345 2002; Lu et al., 2007; Shi et al., 2016). In *C. elegans*, NCA-1 potentiates persistent
346 motor circuit activity and sustains locomotion (Gao et al., 2015).

347 To examine interactions of the *sek-1* p38 MAPK pathway with NCA-1, we tested
348 whether *sek-1* and *nsy-1* mutants suppress the activated NCA-1 mutant *ox352*, referred
349 to as *nca-1(gf)*. The *nca-1(gf)* animals are coiled and uncoordinated; thus, it is difficult to
350 measure their locomotion rate by the body bend assay because they sometimes do not
351 propagate sinusoidal waves down the entire length of their body. Instead, we used a
352 radial locomotion assay in which we placed animals in the center of a 10 cm plate and
353 later measured how far the animals had moved. *nca-1(gf)* double mutants with either
354 *sek-1(km4)* or *nsy-1(ok593)* uncoil a bit but still exhibit uncoordinated locomotion
355 (Figure 5A). In fact, though these double mutants show more movement in the anterior
356 half of their bodies than *nca-1(gf)*, they propagate body waves to their posterior half
357 even more poorly than the *nca-1(gf)* mutant. However, both *sek-1* and *nsy-1* clearly

358 suppress the small size and slow growth rate of the *nca-1(gf)* mutant (Figure 5A) and in
359 radial locomotion assays, *sek-1* and *nsy-1* weakly suppressed the *nca-1(gf)* locomotion
360 phenotype (Figure 5B). Together these data suggest that mutants in the *sek-1* p38
361 MAPK pathway partially suppress some aspects of the *nca-1(gf)* mutant.

362 Given that *sek-1* acts in acetylcholine neurons to regulate wild-type and *egl-*
363 *30(gf)* locomotion, we tested if the same neuron class is responsible for *sek-1*
364 suppression of *nca-1(gf)*. Expression of *sek-1* in all neurons or in acetylcholine neurons
365 of *nca-1(gf) sek-1(km4)* animals restored the *nca-1(gf)* size and posture phenotypes.
366 These worms are small and coiled and closely resemble the *nca-1(gf)* mutant (Figure
367 5C). By contrast, expression of *sek-1* in GABA neurons did not affect the size or posture
368 of the *nca-1(gf) sek-1* double mutant (Figure 5C). These data suggest that *sek-1* acts in
369 acetylcholine neurons to regulate *nca-1(gf)* locomotion. However, in radial locomotion
370 assays, expression of *sek-1* in none of these neuron classes significantly altered the
371 movement of the *nca-1(gf) sek-1* double mutant (Figure 5D), though the weak
372 suppression of *nca-1(gf)* by *sek-1* in this assay makes it difficult to interpret these
373 negative results. We make the tentative conclusion that *sek-1* partially suppresses *nca-*
374 *1(gf)* locomotion and probably acts in the acetylcholine neurons where it also acts to
375 regulate wild-type and *egl-30(gf)* locomotion, suggesting a common neuronal site of
376 action of this pathway.

377

378 **Discussion**

379 In this study we identified a new neuronal role for the mitogen-activated protein
380 kinase kinase SEK-1 and the p38 MAPK pathway as a positive regulator of locomotion

381 and Gq signaling. The p38 MAPK pathway has been best characterized as a pathway
382 activated by a variety of cellular stresses and inflammatory cytokines (Kyriakis and
383 Avruch, 2012), but it has also been implicated in neuronal function, including some
384 forms of mammalian synaptic plasticity (Bolshakov *et al.* 2000; Rush *et al.* 2002; Huang
385 *et al.* 2004). In *C. elegans*, Gq plays a positive role in locomotion by promoting
386 acetylcholine release, so we tested whether the slow locomotion of *sek-1* mutants is
387 directly related to the role of *sek-1* as a regulator of Gq signaling. Through rescue
388 experiments, we found that SEK-1 acts in acetylcholine neurons to regulate both the
389 rate of locomotion and Gq signaling. Previously, *sek-1* has been shown to act in GABA
390 neurons to regulate sensitivity to the acetylcholinesterase inhibitor aldicarb (Vashlishan
391 *et al.*, 2008), and to act in interneurons to regulate trafficking of the GLR-1 glutamate
392 receptor and the frequency of worm reversals (Park and Rongo, 2016). Thus, *sek-1*
393 may play distinct roles in different neuron types. Our data indicate a role for *sek-1* as a
394 positive regulator of Gq signaling in acetylcholine neurons.

395 In addition to SEK-1, we identified other p38 pathway components regulating Gq
396 signaling. Specifically, we found that mutants in *tir-1*, *nsy-1* and a *pmk-1 pmk-2* double
397 mutant exhibit locomotion defects identical to *sek-1* and suppress activated Gq,
398 suggesting that they act in a single p38 pathway to modulate signaling downstream of
399 Gq. These results indicate a redundant function for PMK-1 and PMK-2 in regulating
400 locomotion rate and Gq signaling. PMK-1 and PMK-2 also act redundantly for
401 development of the asymmetric AWC neurons and to regulate induction of serotonin
402 biosynthesis in the ADF neurons in response to pathogenic bacteria (Pagano *et al.*,

403 2015). By contrast, PMK-1 acts alone in the intestine to regulate innate immunity and in
404 interneurons to regulate GLR-1 trafficking (Pagano et al., 2015; Park and Rongo, 2016).

405 What is the downstream effector of *sek-1* p38 MAPK signaling in this Gq
406 signaling pathway? There are several known downstream effectors of p38 MAPK
407 signaling in *C. elegans*, including the transcription factor ATF-7 (Shivers et al., 2010;
408 Inoue et al., 2005; Xie et al., 2013). Our data indicate that ATF-7 is not required for the
409 p38 MAPK-dependent regulation of Gq signaling. It is possible that this p38 MAPK
410 pathway activates molecules other than transcription factors to regulate Gq signaling. It
411 is also possible that the *sek-1* p38 pathway activates multiple downstream effectors that
412 are not individually required.

413 One of the pathways that transduce signals from Gq includes the RhoGEF
414 Trio/UNC-73, the small GTPase Rho, and the cation channel NALCN/NCA-1 (Williams
415 et al., 2007; Topalidou et al., 2016b). We found that mutations in the *sek-1* p38 MAPK
416 pathway partially suppress an activated NCA-1 mutant and that *sek-1* probably acts to
417 control NCA-1 activity in the same neurons where it acts to regulate locomotion and Gq
418 signaling. Given the precedence for direct phosphorylation of sodium channels by p38
419 to regulate channel properties (Wittmack et al., 2005; Hudmon et al., 2008), it is
420 possible that PMK-1 and PMK-2 phosphorylate NCA-1 to regulate its expression,
421 localization, or activity. Our genetic study sets the foundation for further investigation of
422 the specific role of the *sek-1* p38 pathway in the regulation of Gq signaling and NCA-1
423 channel activity.

424

425 **Acknowledgements**

426 We thank Dennis Kim and Chiou-Fen Chuang for strains, Pin-An Chen and Erik
427 Jorgensen for the *nca-1(gf)* mutant *ox352*, Chris Johnson for the fine mapping of *yak42*,
428 Jordan Hoyt for help with Galaxy and CloudMap to analyze WGS data, and Dana Miller
429 for providing access to her microscope camera. Some strains were provided by the
430 CGC, which is funded by NIH Office of Research Infrastructure Programs (P40
431 OD010440). J.M.H was supported in part by Public Health Service, National Research
432 Service Award T32GM007270, from the National Institute of General Medical Sciences.
433 M.A. is an Ellison Medical Foundation New Scholar. This work was supported by NIH
434 grant R00 MH082109 to M.A.

435

436 **Figure Legends**

437 **Figure 1: *sek-1* acts downstream of $G\alpha_q$ to regulate locomotion behavior**

438 (a) Gene structure of *sek-1*. White boxes depict the 5' and 3' untranslated regions, black
439 boxes depict exons, and lines show introns. The positions of the *yak42* and *km4*
440 deletions are shown. *yak42* is a 3713 bp deletion that extends to 1926 bp upstream of
441 the start codon. Drawn with Exon-Intron Graphic Maker
442 (<http://www.wormweb.org/exonintron>). Scale bar is 100 bp.

443 (b) *sek-1(yak42)* and *sek-1(km4)* suppress the small size and loopy waveform of *egl-*
444 *30(tg26)*, written here as *egl-30(gf)*. *unc-82(e1220)* does not suppress *egl-30(gf)*.

445 Photos of first-day adult worms. WT: wild type.

446 (c) *egl-30(gf)* is hyperactive compared to wild-type and suppressed by *sek-1(yak42)* and
447 *sek-1(km4)*. ***, $p < 0.001$, error bars = SEM, $n = 20$.

448 (d) *sek-1* mutant worms have slow locomotion. ***, $p < 0.001$ compared to wild-type, error
449 bars = SEM, $n=20$.

450

451 **Figure 2: *sek-1* acts in mature acetylcholine neurons to regulate locomotion**

452 (A) *sek-1* acts in neurons to regulate locomotion. The *sek-1* wild-type cDNA driven by
453 the *unc-119* pan-neuronal promoter [*unc-119p::sek-1(+)*] rescues the slow locomotion
454 phenotype of *sek-1(km4)* worms. ***, $p < 0.001$, error bars = SEM, $n=20$.

455 (B) *sek-1* acts in acetylcholine neurons to regulate locomotion. *sek-1* WT cDNA driven
456 by the *unc-17* acetylcholine neuron promoter [*unc-17p::sek-1(+)*] rescues the slow
457 locomotion phenotype of *sek-1(km4)* worms but *sek-1* expression in GABA neurons
458 using the *unc-47* promoter [*unc-47p::sek-1(+)*] does not. $p < 0.001$, error bars = SEM,
459 $n=20$.

460 (C-D) *sek-1* acts in acetylcholine neurons to suppress *egl-30(gf)*. Worms expressing
461 *unc-119p::sek-1(+)* or *unc-17p::sek-1(+)* do not have the *egl-30(gf) sek-1* phenotype but
462 worms expressing *unc-47p::sek-1(+)* are identical to *egl-30(gf) sek-1* both for waveform
463 (C) and in the locomotion assay (D). Kruskal-Wallis test, ***, $p < 0.001$, **, $p < 0.01$; error
464 bars = SEM, $n=17-20$.

465 (E) *sek-1* acts in mature neurons to regulate locomotion. *hsp-16.2p::sek-1(+)* rescues
466 the slow locomotion phenotype of *sek-1(km4)*. ***, $p < 0.001$, error bars = SEM, $n=20$.

467

468 **Figure 3: The p38 MAPK pathway regulates locomotion downstream of *egl-30***

469 (A) *tir-1(tm3036)* mutant animals have slow locomotion. ***, $p < 0.001$, error bars = SEM,
470 $n=20$.

471 (B) *tir-1(tm3036)* suppresses *egl-30(gf)*. *egl-30(gf) tir-1* animals move more slowly than
472 the hyperactive *egl-30(gf)* animals. ***, $p < 0.001$, error bars = SEM, $n=20$.

473 (C) *nsy-1(ok593)* mutant animals have slow locomotion. ***, $p < 0.001$, error bars = SEM,
474 $n=20$.

475 (D) *nsy-1(ok593)* suppresses *egl-30(gf)*. *egl-30(gf) nsy-1* animals move more slowly
476 than the hyperactive *egl-30(gf)* animals. ***, $p < 0.001$, error bars = SEM, $n=20$.

477 (E) *pmk-2*, *pmk-2 pmk-1*, and *pmk-3* mutant animals have slow locomotion. ***, $p <$
478 0.001 ; *, $p < 0.05$, compared to WT, error bars = SEM, $n=20$.

479 (F) A *pmk-2 pmk-1* double mutant suppresses the hyperactivity of *egl-30(gf)*. ***, $p <$
480 0.001 , error bars = SEM, $n=20$.

481 (G) A *pmk-2 pmk-1* double mutant suppresses the deep body bends of *egl-30(gf)*. *egl-*
482 *30(gf)* animals with mutations in either *pmk-1*, *pmk-2*, or *pmk-3* are still small and loopy.
483 *egl-30(gf) pmk-2 pmk-1* animals are less loopy and have a more wild-type posture.

484

485 **Figure 4: *sek-1* acts in the same genetic pathway as *unc-73***

486 (A) *sek-1* does not act in the same genetic pathway as *egl-8*. The *sek-1(km4)* mutation
487 enhances the slow locomotion of *egl-8(sa47)* mutants. ***, $p < 0.001$, error bars = SEM,
488 $n=20$.

489 (B) *sek-1* does not act in the same genetic pathway as *rund-1*. The *sek-1(km4)* mutation
490 enhances the slow locomotion of *rund-1(tm3622)* mutants. ***, $p < 0.001$, error bars =
491 SEM, $n=20$.

492 (C) *sek-1* may act in the same genetic pathway as *unc-73*. The *sek-1(km4)* mutation
493 does not enhance the slow locomotion phenotype of *unc-73* mutants. ns, $p > 0.05$, error
494 bars = SEM, $n = 20$.

495 (D) *sek-1(km4)* does not suppress the high-amplitude waveform of *nzIs29 rho-1(gf)*
496 animals. *rho-1(gf)* and *rho-1(gf) sek-1(km4)* animals have similar body posture.

497 (E) *sek-1(km4)* does not suppress the slow locomotion of *rho-1(gf)* animals. ***, $p <$
498 0.001, error bars = SEM, $n = 20$.

499

500 **Figure 5: *sek-1* and *nsy-1* weakly suppress *nca-1(gf)***

501 (a) *nca-1(gf)* mutants are small and tightly coiled. The phenotypes of these *nca-*
502 *1(ox352)* animals are partially suppressed by *nsy-1(ok593)* and *sek-1(km4)*. Photos of
503 first-day adults.

504 (b) *nsy-1* and *sek-1* suppress *nca-1(gf)* locomotion. *nca-1(gf)* animals travel a small
505 distance from the center of the plate in the radial locomotion assay. *nca-1(gf) nsy-*
506 *1(ok593)* and *nca-1(gf) sek-1(km4)* worms move further than *nca-1(gf)* worms. **,
507 $p < 0.01$; *, $p < 0.05$. Error bars = SEM, $n = 30$.

508 (c) Expression of *sek-1* in all neurons and in acetylcholine neurons partially reverts the
509 *sek-1* mutant suppression of *nca-1(gf)* size and body posture. White arrowheads depict
510 food piles created by *nca-1(gf) sek-1(km4)* animals due to their uncoordinated
511 locomotion. Such food piles are not made by *nca-1(gf)* animals.

512 (d) None of the neuronal *sek-1* rescuing constructs revert the radial locomotion
513 phenotype of *nca-1(gf) sek-1(km4)* animals. Although the pan-neuronal and
514 acetylcholine neuron constructs revert the size phenotype of *nca-1(gf) sek-1(km4)*,

515 these animals do not move a significantly different distance than *nca-1(gf) sek-1(km4)*
516 animals. ns, $p > 0.05$. Error bars = SEM, $n = 19-24$.

517

518 **Figure S1: *sek-1* suppresses *egl-30(gf)* deep body bends**

519 (a) *egl-30(gf)* mutants have deeper body bends than wild-type (WT) and *sek-1*
520 mutations suppresses this loopy posture. Images show tracks of forward-moving first-
521 day adults.

522 (b) Quantification of the waveform phenotype. ***, $p < 0.001$, error bars = SEM, $n = 4-5$.

523 (c) *sek-1(ag1)* mutant animals have slow locomotion. ***, $p < 0.001$, error bars = SEM,
524 $n = 10$.

525 (d) *sek-1* suppresses *goa-1* hyperactivity. *goa-1(sa734) sek-1(km4)* animals move more
526 slowly than *goa-1(sa734)* animals. ***, $p < 0.001$, error bars = SEM, $n = 20$.

527

528 **Figure S2: Locomotion of p38 and JNK MAPK pathway mutants**

529 (A) *tir-1(tm3036)* suppresses *egl-30(gf)*. *egl-30(gf) tir-1(tm3036)* animals are less loopy
530 and have a more wild-type posture.

531 (B) *nsy-1(ok593)* suppresses *egl-30(gf)*. *egl-30(gf) nsy-1(ok593)* animals are less loopy
532 and have a more wild-type posture.

533 (C) *jkk-1* and *jnk-1* act in parallel to *sek-1* and *pmk-2 pmk-1*. The *jnk-1(gk7) sek-1(km4)*
534 double mutant and *pmk-2(qd279 qd171) pmk-1(km25) jkk-1(km2)* triple mutants move
535 more slowly than the respective individual mutants. **, $p < 0.01$, *, $p < 0.05$; error bars =
536 SEM, $n = 20$.

537 (D) Worms with gain-of-function or loss-of-function alleles of *atf-7* are slower than wild-
538 type worms. $p < 0.001$, error bars = SEM, $n=20$.

539 (E) Worms lacking *gap-2* and *vhp-1* move like wild-type worms. Neither *gap-2(tm478)*
540 nor *vhp-1(sa366)* confers a slow locomotion phenotype. ns, $p > 0.05$ compared to WT,
541 error bars = SEM, $n=20$.

542 (F-G) *tir-1(ky648gf)* animals do not have loopy or hyperactive locomotion. *tir-1(ky648gf)*
543 worms have wild-type posture and are slower than wild-type animals. ***, $p < 0.001$,
544 error bars = SEM, $n=20$.

545

546 **Table S1: Strain List**

Strain	Genotype
AU1	<i>sek-1(ag1)</i> X
BS3383	<i>pmk-3(ok169)</i> IV
CX3695	<i>kyls140[<i>str-2p::gfp</i>, <i>lin-15(+)</i>]</i> I
CX5959	<i>kyls140[<i>str-2p::gfp</i>, <i>lin-15(+)</i>]</i> I; <i>tir-1(ky648gf)</i> III
EG317	<i>unc-73(ox317)</i> I
EG1000	<i>dpy-5(e61)</i> I; <i>rol-6(e187)</i> II; <i>lon-1(e1820)</i> III
EG1020	<i>bli-6(sc16)</i> IV; <i>dpy-11(e224)</i> V; <i>lon-2(e678)</i> X
EG4782	<i>nzls29[<i>unc-17p::rho-1(G14V)</i>, <i>unc-122::gfp</i>]</i> II
EG5505	<i>rund-1(tm3622)</i> X
EG7989	<i>unc-119(ed3)</i> III; <i>oxTi668[<i>eft-3p::TdTomato::H2B</i>, <i>Cb-unc-119(+)</i>]</i> X
IG685	<i>tir-1(tm3036)</i> III
JN147	<i>gap-2(tm748)</i> X

JT47	<i>egl-8(sa47)</i> V
JT366	<i>vhp-1(sa366)</i> II
JT734	<i>goa-1(sa734)</i> I
KU2	<i>jkk-1(km2)</i> X
KU4	<i>sek-1(km4)</i> X
KU25	<i>pmk-1(km25)</i> IV
N2	Bristol wild isolate, standard lab wild-type
VC8	<i>jnk-1(gk7)</i> IV
VC390	<i>nsy-1(ok593)</i> IV
XZ42	<i>sek-1(yak42)</i> X
XZ1233	<i>egl-30(tg26)</i> I; <i>sek-1(yak42)</i> X
XZ1151	<i>egl-30(tg26)</i> I
XZ1566	<i>egl-8(sa47)</i> V; <i>sek-1(yak42)</i> X
XZ1567	<i>unc-73(ox317)</i> I; <i>sek-1(yak42)</i> X
XZ1574	<i>rund-1(tm3622)</i> <i>sek-1(yak42)</i> X
XZ1575	<i>egl-30(tg26)</i> I; <i>sek-1(km4)</i> X
XZ1588	<i>egl-30(tg26)</i> I; <i>nsy-1(ok593)</i> IV
XZ1589	<i>egl-30(tg26)</i> I; <i>sek-1(km4)</i> X; <i>qdEx8[unc-119p::sek-1::GFP, myo-2p::mStrawberry::unc-54-3'UTR]</i>
XZ1593	<i>egl-30(tg26)</i> I; <i>pmk-1(km25)</i> IV
XZ1642	<i>sek-1(km4)</i> X; <i>yakEx72[unc-17p::sek-1::tbb-2utr-operon-GFP::H2B::cye-1utr, myo-2p::mCherry]</i>
XZ1643	<i>sek-1(km4)</i> X; <i>yakEx73[unc-47p::sek-1::tbb-2utr-operon-GFP::H2B::cye-</i>

	<i>1utr, myo-2p::mCherry]</i>
XZ1717	<i>nzls29[unc-17p::rho-1(G14V) unc-122::gfp] II; sek-1(km4) X</i>
XZ1770	<i>egl-30(tg26) I; pmk-2(qd279 qd171) pmk-1(km25) IV</i>
XZ1771	<i>egl-30(tg26) I; pmk-2(qd287) IV</i>
XZ1772	<i>egl-30(tg26) I; pmk-3(ok169) IV</i>
XZ1815	<i>egl-30(tg26) I; tir-1(tm3036) III</i>
XZ1816	<i>nca-1(ox352) IV; sek-1(km4) X; qdEx8[unc-119p::sek-1::GFP::unc-54-3' UTR, myo-2p::mStrawberry::unc-54-3'UTR]</i>
XZ1834	<i>egl-30(tg26) I; sek-1(km4) X; yakEx72[unc-17p::sek-1::tbb-2utr-operon-GFP::H2B::cye-1utr, myo-2p::mCherry]</i>
XZ1835	<i>nca-1(ox352) IV; sek-1(km4) X; yakEx72[unc-17p::sek-1::tbb-2utr-operon-GFP::H2B::cye-1utr, myo-2p::mCherry]</i>
XZ1861	<i>nca-1(ox352) IV; sek-1(km4) X; yakEx73[unc-47p::sek-1::tbb-2utr-operon-GFP::H2B::cye-1utr, myo-2p::mCherry]</i>
XZ1863	<i>egl-30(tg26) I; sek-1(km4) X; yakEx73[unc-47p::sek-1::tbb-2utr-operon-GFP::H2B::cye-1utr, myo-2p::mCherry]</i>
XZ1872	<i>jnk-1(gk7) I; sek-1(km4) X</i>
XZ1873	<i>pmk-2(qd279 qd171) pmk-1(km25) IV; jkk-1(km2) X</i>
XZ1937	<i>sek-1(km4) X; yakEx121[hsp-16.2p::sek-1::tbb-2-3' UTR::gld-1 operon linker::gfp::h2b, myo-2p::mCherry]</i>
XZ1939	<i>goa-1(sa734) I; sek-1(km4) X</i>
XZ1942	<i>tir-1(ky648gf) III</i>
ZD202	<i>sek-1(km4) X; qdEx8[unc-119p::sek-1::GFP::unc-54-3' UTR + myo-</i>

	<i>2p::mStrawberry::unc-54-3'UTR]</i>
ZD318	<i>agls29 atf-7(qd22 qd130) III</i>
ZD442	<i>agls29 atf-7(qd22) III</i>
ZD934	<i>pmk-2(qd279 qd171) pmk-1(km25) IV</i>
ZD1020	<i>pmk-2(qd287) IV</i>

547

548 **Table S2: Plasmids and Primers**

549 Gateway entry clones

Plasmid	Details
pJH21	<i>sek-1</i> cDNA [1-2]
pCFJ150	pDEST5605[4-3]
pCFJ326	<i>tbb-2utr-operon-GFP::H2B::cye-1utr</i> [2-3]
pMH522	<i>unc-47p</i> [4-1]
pGH1	<i>unc-17p</i> [4-1]
pCM1.56	<i>hsp-16.2p</i> [4-1]

550

551 Gateway Expression Constructs

Plasmid	Details	Used to make
pJH23	<i>unc-17p::sek-1:: tbb-2utr-operon-GFP::H2B::cye-1utr</i>	<i>yakEx72</i>
pJH24	<i>unc-47p::sek-1:: tbb-2utr-operon-GFP::H2B::cye-1utr</i>	<i>yakEx73</i>
pJH46	<i>hsp-16.2p::sek-1:: tbb-2utr-</i>	<i>yakEx121</i>

	<i>operon-GFP::H2B::cye-1utr</i>	
--	----------------------------------	--

552

553 Primers

oJH114	GGGGACAAGTTTGTACAAAAAAGCA GGCTcaATGGAGCGAAAAGGACGT G	F to clone <i>sek-1</i> cDNA into [1-2]
oJH115	GGGGACCACTTTGTACAAGAAAGCT GGGTgTCATCGTCGCCAAACAGTG	R to clone <i>sek-1</i> cDNA into [1-2]

554

555

556 **Table S3: Statistical Tests**

Figure	Test	p value
1C	One-way ANOVA and Bonferroni's Multiple Comparison Test WT vs <i>egl-30(tg26)</i> (p<0.001) <i>egl-30(tg26)</i> vs <i>egl-30(tg26); sek-1(yak42)</i> (p<0.001) <i>egl-30(tg26)</i> vs <i>egl-30(tg26);sek-1(km4)</i> (p<0.001)	< 0.001
1D	One-way ANOVA and Dunnett's Multiple Comparison Test WT vs <i>sek-1(yak42)</i> (p<0.001) WT vs <i>sek-1(km4)</i> (p<0.001)	< 0.001

2A	One-way ANOVA and Bonferroni's Multiple Comparison Test <i>sek-1(km4)</i> vs <i>sek-1(km4)</i> ; <i>qdEx8[unc-119p::sek-1(+)]</i> (p<0.001)	< 0.001
2B	One-way ANOVA and Bonferroni's Multiple Comparison Test <i>sek-1(km4)</i> vs <i>sek-1(km4)</i> ; <i>yakEx72[unc-17p::sek-1(+)]</i> (p<0.001) <i>sek-1(km4)</i> vs <i>sek-1(km4)</i> ; <i>yakEx73[unc-47p::sek-1(+)]</i> (ns)	< 0.001
2D	Kruskal-Wallis Test and Dunn's Multiple Comparison Test <i>egl-30(tg26)</i> ; <i>sek-1(km4)</i> vs <i>egl-30(tg26)</i> ; <i>sek-1(km4)</i> ; <i>qdEx8[unc-119p::sek-1(+)]</i> (p<0.001) <i>egl-30(tg26)</i> ; <i>sek-1(km4)</i> vs <i>egl-30(tg26)</i> ; <i>sek-1(km4)</i> ; <i>yakEx72[unc-17p::sek-1(+)]</i> (p<0.01) <i>egl-30(tg26)</i> ; <i>sek-1(km4)</i> vs <i>egl-30(tg26)</i> ; <i>sek-1(km4)</i> ; <i>yakEx73[unc-47p::sek-1(+)]</i> (ns)	< 0.001
2E	One-way ANOVA and Bonferroni's Multiple Comparison Test <i>sek-1(km4)</i> vs <i>sek-1(km4)</i> ; <i>yakEx121[hsp-16.2p::sek-1(+)]</i> (p<0.001)	< 0.001
3A	Unpaired t test, two-tailed	< 0.001

3B	One-way ANOVA and Bonferroni's Multiple Comparison Test <i>egl-30(tg26) vs egl-30(tg26); tir-1(tm3036)</i> (p<0.001)	< 0.001
3C	Unpaired t test, two-tailed	< 0.001
3D	One-way ANOVA and Bonferroni's Multiple Comparison Test <i>egl-30(tg26) vs egl-30(tg26); nsy-1(ok593)</i> (p<0.001)	< 0.001
3E	One-way ANOVA and Dunnett's Multiple Comparison Test WT vs <i>pmk-1(km25)</i> (ns) WT vs <i>pmk-2(qd287)</i> (p<0.05) WT vs <i>pmk-2(qd279 qd171) pmk-1 (km25)</i> (p<0.001) WT vs <i>pmk-3(ok169)</i> (p<0.001)	< 0.001
3F	One-way ANOVA and Dunnett's Multiple Comparison Test <i>egl-30(tg26) vs egl-30(tg26); pmk-1(km25)</i> (p<0.001) <i>egl-30(tg26) vs egl-30(tg26); pmk-2(qd287)</i> (p<0.001) <i>egl-30(tg26) vs egl-30(tg26); pmk-2(qd279 qd171) pmk-1 (km25)</i> (p<0.001) <i>egl-30(tg26) vs egl-30(tg26); pmk-3(ok169)</i> (p<0.001)	< 0.001
4A	One-way ANOVA and Bonferroni's Multiple Comparison Test <i>egl-8(sa47) vs egl-8(sa47); sek-1(yak42)</i> (p<0.001)	< 0.001
4B	One-way ANOVA and Bonferroni's Multiple Comparison Test	< 0.001

	<i>sek-1(yak42)</i> vs <i>rund-1(tm3622)</i> ; <i>sek-1(yak42)</i> (p<0.001)	
4C	One-way ANOVA and Bonferroni's Multiple Comparison Test <i>unc-73(ox317)</i> vs <i>unc-73(ox317)</i> ; <i>sek-1(yak42)</i> (ns)	< 0.001
4E	One-way ANOVA and Bonferroni's Multiple Comparison Test <i>nzls29[unc-17p::rho-1(G14V)]</i> vs <i>nzls29[unc-17p::rho-1(G14V)]</i> ; <i>sek-1(km4)</i> (p<0.001)	< 0.001
5B	One-way ANOVA and Bonferroni's Multiple Comparison Test WT vs <i>nca-1(ox352)</i> (p<0.001) <i>nca-1(ox352)</i> vs <i>nca-1(ox352)</i> ; <i>nsy-1(ok593)</i> (p<0.01) <i>nca-1(ox352)</i> vs <i>nca-1(ox352)</i> ; <i>sek-1(km4)</i> (p<0.05)	< 0.001
5D	Kruskal-Wallis Test and Dunn's Multiple Comparison Test <i>nca-1(ox352);sek-1(km4)</i> vs <i>nca-1(ox352);sek-1(km4)</i> ; <i>qdEx8[unc-119p::sek-1(+)]</i> (ns) <i>nca-1(ox352);sek-1(km4)</i> vs <i>nca-1(ox352);sek-1(km4)</i> ; <i>yakEx72[unc-17p::sek-1(+)]</i> (ns) <i>nca-1(ox352);sek-1(km4)</i> vs <i>nca-1(ox352);sek-1(km4)</i> ; <i>yakEx73[unc-47p::sek-1(+)]</i> (ns)	< 0.001
S1B	One-way ANOVA and Bonferroni's Multiple Comparison Test <i>egl-30(tg26)</i> vs <i>egl-30(tg26)</i> ; <i>sek-1(yak42)</i>	< 0.001

	(p<0.001) <i>egl-30(tg26)</i> vs <i>egl-30(tg26); sek-1(km4)</i> (p<0.001)	
S1C	One-way ANOVA and Newman-Keuls Multiple Comparison Test WT vs <i>sek-1(yak42)</i> (p<0.001) WT vs <i>sek-1(ag1)</i> (p<0.001) <i>sek-1(yak42)</i> vs <i>sek-1(ag1)</i> (ns)	< 0.001
S1D	One-way ANOVA and Bonferroni's Multiple Comparison Test WT vs <i>sek-1(km4)</i> (p<0.001) <i>goa-1(sa734)</i> vs <i>sek-1(km4)</i> (p<0.001) <i>goa-1(sa734); sek-1(km4)</i> vs <i>sek-1(km4)</i> (p<0.001)	< 0.001
S2C	One-way ANOVA and Bonferroni's Multiple Comparison Test <i>jnk-1(gk7)</i> vs <i>jnk-1(gk7); sek-1(km4)</i> (p<0.01) <i>jkk-1(km2)</i> vs <i>pmk-2(qd279 qd171) pmk-1 (km25); jkk-1(km2)</i> (p<0.05)	< 0.001
S2D	One-way ANOVA and Bonferroni's Multiple Comparison Test WT vs <i>atf-7(qd22)</i> (p<0.001) WT vs <i>atf-7(qd22 qd130)</i> (p<0.001)	< 0.001
S2E	One-way ANOVA	p=0.806

S2G	Unpaired t test, two-tailed	< 0.001
-----	-----------------------------	---------

557

558 **References**

559 Ailion, M., M. Hannemann, S. Dalton, A. Pappas, S. Watanabe, *et al.*, 2014 Two Rab2
560 interactors regulate dense-core vesicle maturation. *Neuron* 82: 167–180.

561 Andrusiak, M. G., and Y. Jin, 2016 Context Specificity of Stress-activated Mitogen-
562 activated Protein (MAP) Kinase Signaling: The Story as Told by *Caenorhabditis*
563 *elegans*. *J. Biol. Chem.* 291: 7796–7804.

564 Bastiani, C. A., S. Gharib, M. I. Simon, and P. W. Sternberg, 2003 *Caenorhabditis*
565 *elegans* Gαq Regulates Egg-Laying Behavior via a PLCβ-Independent and Serotonin-
566 Dependent Signaling Pathway and Likely Functions Both in the Nervous System and in
567 Muscle. *Genetics* 165: 1805–1822.

568 Bence, K., W. Ma, T. Kozasa, and X. -Y. Huang, 1997 Direct stimulation of Bruton's
569 tyrosine kinase by Gq-protein α-subunit. *Nature* 389: 296–299.

570 Bolshakov V. Y., Carboni L., Cobb M. H., Siegelbaum S. A., Belardetti F., 2000 Dual
571 MAP kinase pathways mediate opposing forms of long-term plasticity at CA3-CA1
572 synapses. *Nat. Neurosci.* **3**: 1107–1112.

573 Brenner, S., 1974 The genetics of *Caenorhabditis elegans*. *Genetics* 77: 71–94.

574 Chang, C., Y. -W. Hsieh, B. J. Lesch, C. I. Bargmann, and C. -F. Chuang, 2011
575 Microtubule-based localization of a synaptic calcium-signaling complex is required for
576 left-right neuronal asymmetry in *C. elegans*. *Development* 138: 3509–3518.

- 577 Chuang, C. -F., and C. I. Bargmann, 2005 A Toll-interleukin 1 repeat protein at the
578 synapse specifies asymmetric odorant receptor expression via ASK1 MAPKKK
579 signaling. *Genes Dev.* 19: 270–281.
- 580 Couillault, C., N. Pujol, J. Reboul, L. Sabatier, J. -F. Guichou, *et al.*, 2004 TLR-
581 independent control of innate immunity in *Caenorhabditis elegans* by the TIR domain
582 adaptor protein TIR-1, an ortholog of human SARM. *Nat. Immunol.* 5: 488–494.
- 583 Doi, M., and K. Iwasaki, 2002 Regulation of Retrograde Signaling at Neuromuscular
584 Junctions by the Novel C2 Domain Protein AEX-1. *Neuron* 33: 249–259.
- 585 Fay, D. 2006 Genetic mapping and manipulation: Chapter 7-Making compound
586 mutants. *WormBook*, ed. The *C. elegans* Research Community, WormBook,
587 doi/10.1895/wormbook.1.96.2, <http://www.wormbook.org>
- 588 Frøkjær-Jensen, C., M. W. Davis, M. Ailion, and E. M. Jorgensen 2012 Improved Mos1-
589 mediated transgenesis in *C. elegans*. *Nat. Methods* 9: 117–118.
- 590 Frøkjær-Jensen, C., M. W. Davis, M. Sarov, J. Taylor, S. Flibotte, *et al.*, 2014 Random
591 and targeted transgene insertion in *C. elegans* using a modified Mos1 transposon. *Nat.*
592 *Methods* 11: 529–534.
- 593 Gao, S., L. Xie, T. Kawano, M. D. Po, J. K. Pirri, *et al.*, 2015 The NCA sodium leak
594 channel is required for persistent motor circuit activity that sustains locomotion. *Nat.*
595 *Commun.* 6: 6323.

- 596 García-Hoz, C., G. Sánchez-Fernández, M. T. Díaz-Mec, J. Moscat, F. Mayor *et al.*,
597 2010 Gαq Acts as an Adaptor Protein in Protein Kinase Cζ (PKCζ)-mediated ERK5
598 Activation by G Protein-coupled Receptors (GPCR). *J. Biol. Chem.* 285: 13480–13489.
- 599 Hajdu-Cronin, Y. M., W. J. Chen, G. Patikoglou, M. R. Koelle, and P. W. Sternberg,
600 1999 Antagonism between Gαα and Gαq in *Caenorhabditis elegans*: the RGS protein
601 EAT-16 is necessary for Gαα signaling and regulates Gαq activity. *Genes Dev.* 13:
602 1780–1793.
- 603 Hoppe, P. E., J. Chau, K. A. Flanagan, A. R. Reedy, and L. A. Schriefer, 2010
604 *Caenorhabditis elegans unc-82* Encodes a Serine/Threonine Kinase Important for
605 Myosin Filament Organization in Muscle During Growth. *Genetics* 184: 79–90.
- 606 Huang, C. -C., J. -L. You, M. -Y. Wu, and K. -S. Hsu, 2004 Rap1-induced p38 mitogen-
607 activated protein kinase activation facilitates AMPA receptor trafficking via the
608 GDI.Rab5 complex. Potential role in (S)-3,5-dihydroxyphenylglycine-induced long term
609 depression. *J. Biol. Chem.* 279: 12286–12292.
- 610 Hudmon, A., J. -S. Choi, L. Tyrrell, J. A. Black, A. M. Rush, *et al.*, 2008 Phosphorylation
611 of Sodium Channel Nav1.8 by p38 Mitogen-Activated Protein Kinase Increases Current
612 Density in Dorsal Root Ganglion Neurons. *J. Neurosci.* 28: 3190–3201.
- 613 Inoue, H., N. Hisamoto, J. H. An, R. P. Oliveira, E. Nishida, *et al.*, 2005 The *C. elegans*
614 p38 MAPK pathway regulates nuclear localization of the transcription factor SKN-1 in
615 oxidative stress response. *Genes Dev.* 19: 2278–2283.

616 Jantsch-Plunger, V., P. Gönczy, A. Romano, H. Schnabel, D. Hamill, *et al.*, 2000 CYK-
617 4: A Rho family gtpase activating protein (GAP) required for central spindle formation
618 and cytokinesis. *J. Cell Biol.* 149: 1391–1404.

619 Kawasaki, M., N. Hisamoto, Y. Iino, M. Yamamoto, J. Ninomiya-Tsuji, *et al.*, 1999 A
620 *Caenorhabditis elegans* JNK signal transduction pathway regulates coordinated
621 movement via type-D GABAergic motor neurons. *EMBO J.* 18: 3604–3615.

622 Kim, D.H., R. Feinbaum, G. Alloing, F. E. Emerson, D. A. Garsin, *et al.*, 2002 A
623 Conserved p38 MAP Kinase Pathway in *Caenorhabditis elegans* Innate Immunity.
624 *Science* 297: 623–626.

625 Kim, D.H., N. T. Liberati, T. Mizuno, H. Inoue, N. Hisamoto, *et al.*, 2004 Integration of
626 *Caenorhabditis elegans* MAPK pathways mediating immunity and stress resistance by
627 MEK-1 MAPK kinase and VHP-1 MAPK phosphatase. *Proc. Natl. Acad. Sci. U. S. A.*
628 101: 10990–10994.

629 Koelle, M. R., 2016 Neurotransmitter signaling through heterotrimeric G proteins:
630 insights from studies in *C. elegans*. *WormBook*, doi:10.1895/wormbook.1.75.2.

631 Kyriakis, J. M., and J. Avruch, 2012 Mammalian MAPK signal transduction pathways
632 activated by stress and inflammation: a 10-year update. *Physiol. Rev.* 92:689-737.

633 Lackner, M. R., S. J. Nurrish, and J. M. Kaplan, 1999 Facilitation of Synaptic
634 Transmission by EGL-30 Gq α and EGL-8 PLC β : DAG Binding to UNC-13 Is Required to
635 Stimulate Acetylcholine Release. *Neuron* 24: 335–346.

- 636 Lu, B., Y. Su, S. Das, J. Liu, J. Xia, *et al.*, 2007 The Neuronal Channel NALCN
637 Contributes Resting Sodium Permeability and Is Required for Normal Respiratory
638 Rhythm. *Cell* 129: 371–383.
- 639 McMullan, R., E. Hiley, P. Morrison, and S. J. Nurrish 2006 Rho is a presynaptic
640 activator of neurotransmitter release at pre-existing synapses in *C. elegans*. *Genes*
641 *Dev.* 20: 65–76.
- 642 Mello, C. C., J. M. Kramer, D. Stinchcomb, and V. Ambros, 1991 Efficient gene transfer
643 in *C.elegans*: extrachromosomal maintenance and integration of transforming
644 sequences. *EMBO J.* 10: 3959–3970.
- 645 Miller, K. G., M. D. Emerson, and J. B. Rand 1999 $G\alpha$ and Diacylglycerol Kinase
646 Negatively Regulate the $Gq\alpha$ Pathway in *C. elegans*. *Neuron* 24: 323–333.
- 647 Minevich, G., D. S. Park, D. Blankenberg, R. J. Poole, and O. Hobert, 2012 CloudMap:
648 a cloud-based pipeline for analysis of mutant genome sequences. *Genetics* 192: 1249–
649 1269.
- 650 Nash, H. A., R. L. Scott, B. C. Lear, and R. Allada, 2002 An unusual cation channel
651 mediates photic control of locomotion in *Drosophila*. *Curr. Biol.* 12: 2152–2158.
- 652 Nurrish S., Ségalat L., Kaplan J. M., 1999 Serotonin inhibition of synaptic transmission:
653 $G\alpha(0)$ decreases the abundance of UNC-13 at release sites. *Neuron* 24: 231–242.

- 654 Pagano, D. J., E. R. Kingston, and D. H. Kim, 2015 Tissue Expression Pattern of PMK-2
655 p38 MAPK Is Established by the miR-58 Family in *C. elegans*. PLOS Genet 11:
656 e1004997.
- 657 Park, E.C., and Rongo, C. (2016). The p38 MAP kinase pathway modulates the hypoxia
658 response and glutamate receptor trafficking in aging neurons. eLife 5, e12010.
- 659 Plowman, G. D., S. Sudarsanam, J. Bingham, D. Whyte, and T. Hunter, 1999 The
660 protein kinases of *Caenorhabditis elegans*: a model for signal transduction in
661 multicellular organisms. Proc. Natl. Acad. Sci. U. S. A. 96: 13603–13610.
- 662 Rhee, S. G. 2001 Regulation of Phosphoinositide-Specific Phospholipase C. Annu. Rev.
663 Biochem. 70: 281–312.
- 664 Rush A. M., Wu J., Rowan M. J., Anwyl R., 2002 Group I metabotropic glutamate
665 receptor (mGluR)-dependent long-term depression mediated via p38 mitogen-activated
666 protein kinase is inhibited by previous high-frequency stimulation and activation of
667 mGluRs and protein kinase C in the rat dentate gyrus in vitro. J. Neurosci. 22: 6121–
668 6128.
- 669 Sagasti, A., N. Hisamoto, J. Hyodo, M. Tanaka-Hino, K. Matsumoto, *et al.*, (2001). The
670 CaMKII UNC-43 Activates the MAPKKK NSY-1 to Execute a Lateral Signaling Decision
671 Required for Asymmetric Olfactory Neuron Fates. Cell 105: 221–232.
- 672 Sánchez-Fernández, G., S. Cabezudo, C. García-Hoz, C. Benincá, A. M. Aragay, *et al.*,
673 (2014). Gαq signalling: The new and the old. Cell. Signal. 26: 833–848.

- 674 Shi, Y., C. Abe, B. B. Holloway, S. Shu, N. N. Kumar, *et al.*, 2016 Nalc1 Is a “Leak”
675 Sodium Channel That Regulates Excitability of Brainstem Chemosensory Neurons and
676 Breathing. *J. Neurosci.* 36: 8174–8187.
- 677 Shivers, R. P., D. J. Pagano, T. Kooistra, C. E. Richardson, K. C. Reddy, *et al.*, 2010
678 Phosphorylation of the conserved transcription factor ATF-7 by PMK-1 p38 MAPK
679 regulates innate immunity in *Caenorhabditis elegans*. *PLoS Genet.* 6: e1000892.
- 680 Tanaka-Hino, M., A. Sagasti, N. Hisamoto, M. Kawasaki, S. Nakano, *et al.*, 2002 SEK-1
681 MAPKK mediates Ca²⁺ signaling to determine neuronal asymmetric development in
682 *Caenorhabditis elegans*. *EMBO Rep.* 3: 56–62.
- 683 Topalidou, I., J. Cattin-Ortolá, A. L. Pappas, K. Cooper, G. E. Merrihew, *et al.*, 2016a
684 The EARP Complex and Its Interactor EIPR-1 Are Required for Cargo Sorting to Dense-
685 Core Vesicles. *PLOS Genet* 12: e1006074.
- 686 Topalidou I., Chen P.-A., Cooper K., Watanabe S., Jorgensen E. M., *et al.*, 2016b The
687 NCA-1 ion channel functions downstream of Gq and Rho to regulate locomotion in *C.*
688 *elegans*. bioRxiv. doi: <http://dx.doi.org/10.1101/090514>
- 689 Vaqué, J. P., R. T. Dorsam, X. Feng, R. Iglesias-Bartolome, D. J. Forsthoefel, *et al.*,
690 2013 A genome-wide RNAi screen reveals a Trio-regulated Rho GTPase circuitry
691 transducing mitogenic signals initiated by G protein-coupled receptors. *Mol. Cell* 49: 94–
692 108.
- 693 Vashlishan, A. B., J. M. Madison, M. Dybbs, M., J. Bai, D. Sieburth, *et al.*, 2008 An
694 RNAi Screen Identifies Genes that Regulate GABA Synapses. *Neuron* 58: 346–361.

695 Williams, S. L., S. Lutz, N. K. Charlie, C. Vettel, M. Ailion, *et al.*, 2007 Trio's Rho-
696 specific GEF domain is the missing Galpha q effector in *C. elegans*. *Genes Dev.* 21:
697 2731–2746.

698 Wittmack, E. K., A. M. Rush, A. Hudmon, S. G. Waxman, and S. D. Dib-Hajj, 2005
699 Voltage-Gated Sodium Channel Nav1.6 Is Modulated by p38 Mitogen-Activated Protein
700 Kinase. *J. Neurosci.* 25: 6621–6630.

701 Xie, Y., M. Moussaif, S. Choi, L. Xu, and J. Y. Sze, 2013 RFX transcription factor DAF-
702 19 regulates 5-HT and innate immune responses to pathogenic bacteria in
703 *Caenorhabditis elegans*. *PLoS Genet.* 9: e1003324.

704 Zhang, R., X. He, W. Liu, M. Lu, J. -T. Hsieh, *et al.*, 2003 AIP1 mediates TNF- α -
705 induced ASK1 activation by facilitating dissociation of ASK1 from its inhibitor 14-3-3. *J.*
706 *Clin. Invest.* 111: 1933–1943.

707

Figure 1

bioRxiv preprint doi: <https://doi.org/10.1101/093252>; this version posted December 13, 2016. The copyright holder for this preprint (which was not certified by peer review) is the author/funder, who has granted bioRxiv a license to display the preprint in perpetuity. It is made available under aCC-BY-NC 4.0 International license.

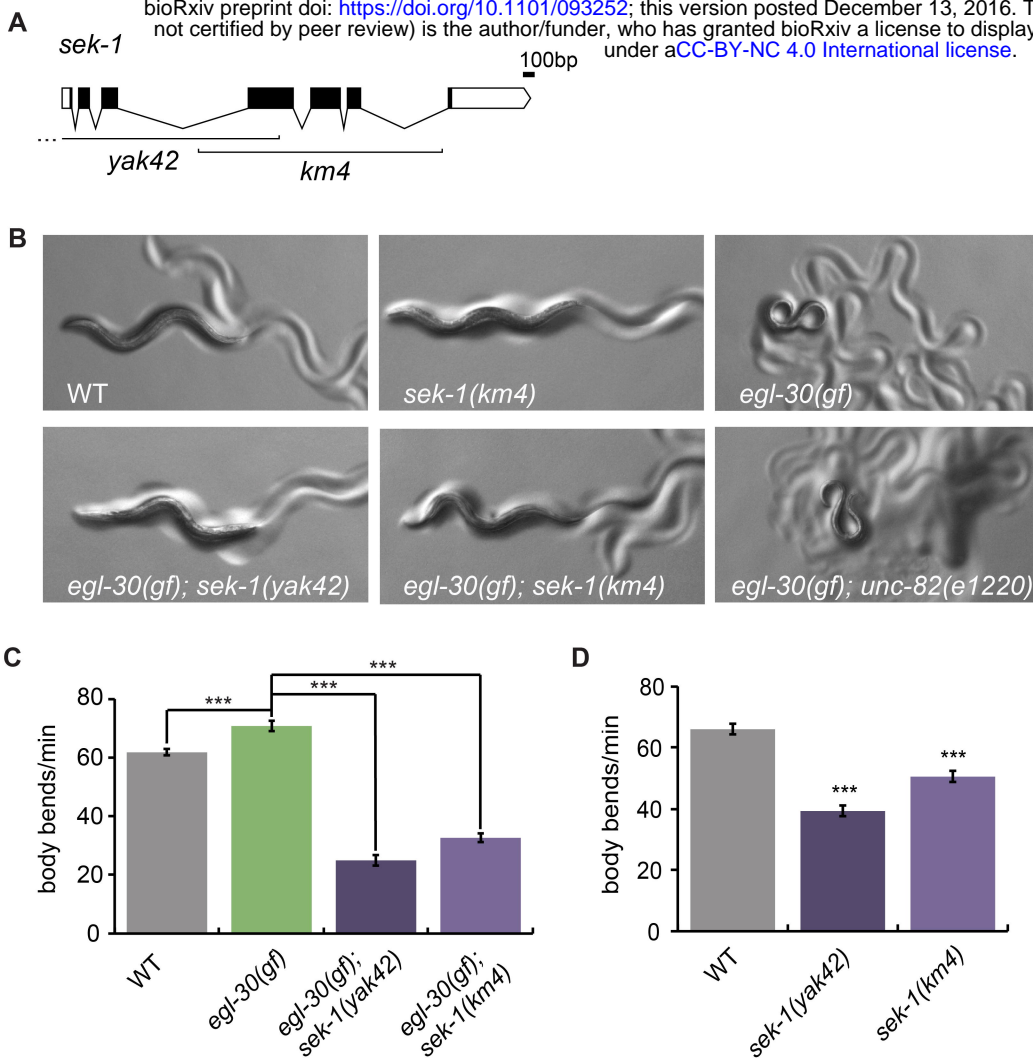


Figure 2

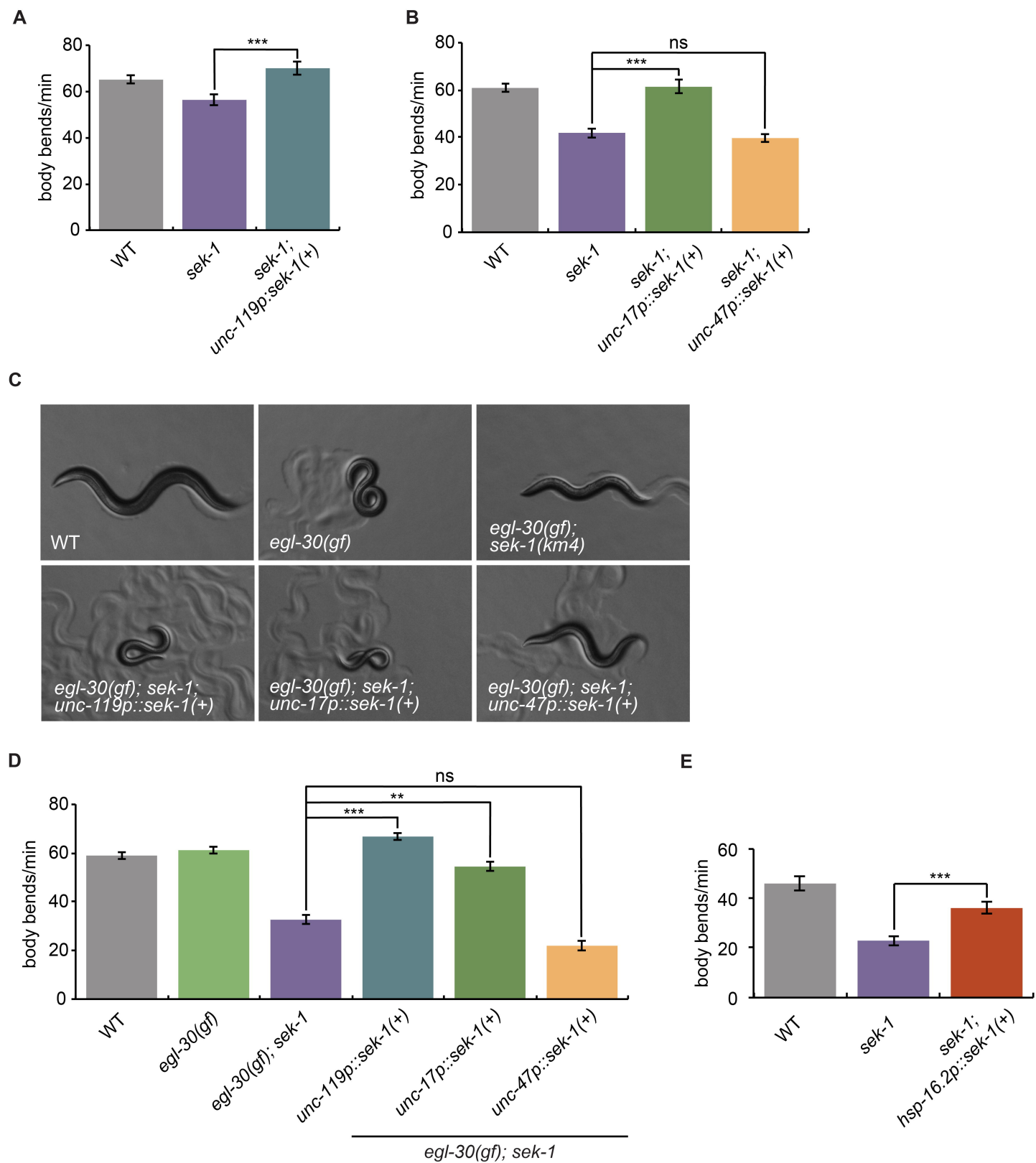


Figure 3

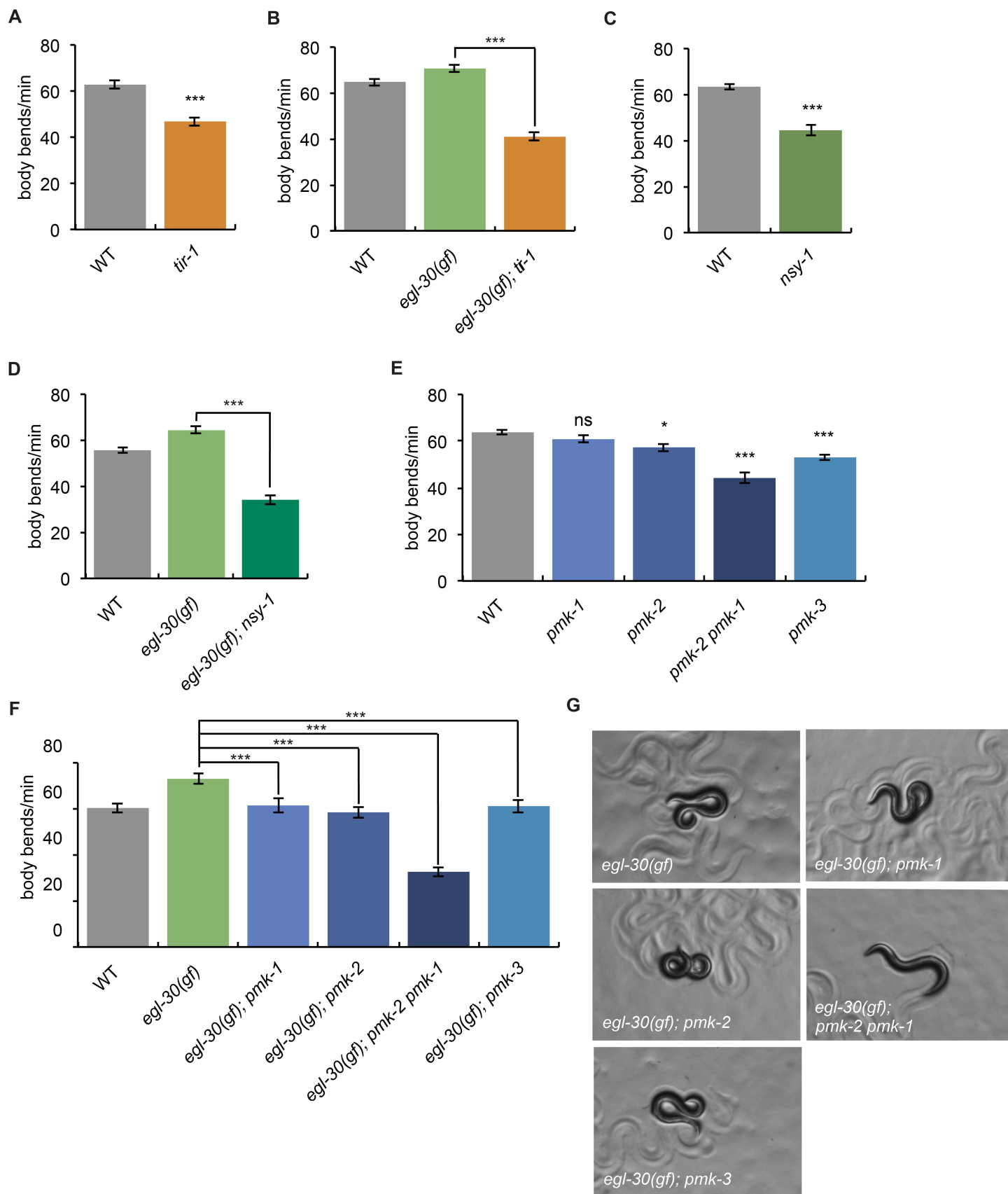


Figure 4

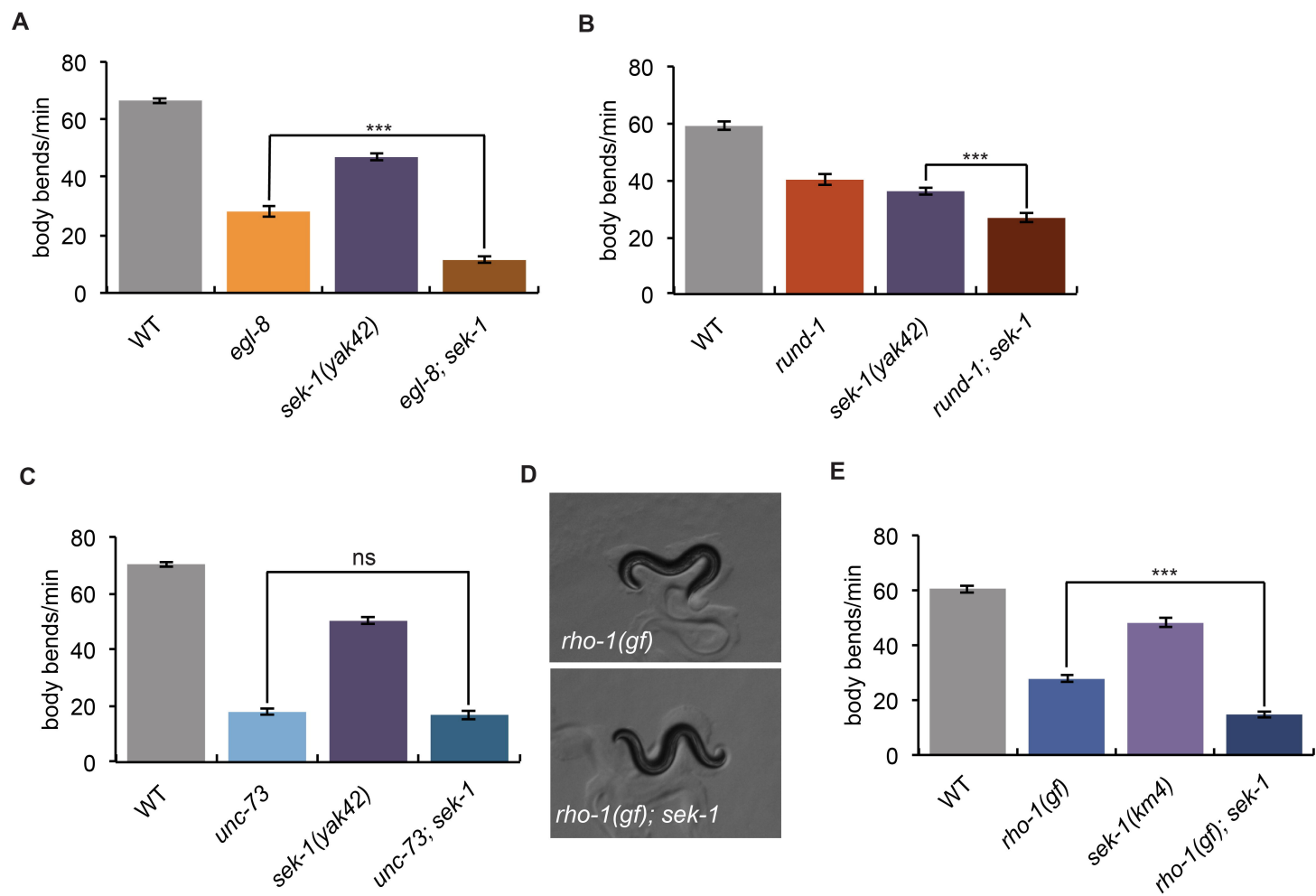


Figure 5

